

# Accurate Molecular Electrostatic Potentials Based on Modified PRDDO/M Wave Functions: III. Extension of the *PESP* Method for Calculation of Electrostatic Potential-Derived Atomic Charges to Compounds Containing $\text{Li}^+$ , $\text{Na}^+$ , $\text{Mg}^{2+}$ , $\text{K}^+$ , $\text{Ca}^{2+}$ , $\text{Zn}^{2+}$ , and I

DENNIS S. MARYNICK

Valerian Software, 3058 Creekview Drive, Grapevine, Texas 76051

Received 16 December 1997; accepted 15 April 1998

**ABSTRACT:** The *PESP* (Parameterized ElectroStatic Potential) method for calculating molecular electrostatic potentials, previously parameterized for H, C, N, O, F, P, S, Cl, and Br, is extended to molecules containing  $\text{Li}^+$ ,  $\text{Na}^+$ ,  $\text{Mg}^{2+}$ ,  $\text{K}^+$ ,  $\text{Ca}^{2+}$ ,  $\text{Zn}^{2+}$ , and I. For a collection of 166 molecules containing 1668 atoms with at least one metal or iodine atom, *PESP* achieves an average absolute deviation in electrostatic potential-derived atomic charges of  $0.042e^-$  compared with *ab initio* MP2/6-31G\*\* calculations, with a correlation coefficient of 0.996. For a larger data set, consisting of 311 molecules encompassing all of the 16 elements just listed (2488 total atoms), *PESP* achieves an average absolute deviation of  $0.040e^-$  and a correlation coefficient of 0.995. *PESP* calculations are an order of magnitude faster than the simplest *ab initio* method (STO-3G) on large molecules, while achieving a level of accuracy that rivals much more elaborate *ab initio* methods. © 1998 John Wiley & Sons, Inc. J Comput Chem 19: 1456–1469, 1998

**Keywords:** electrostatic; potential; PRDDO; *PESP*

## Introduction

The molecular electrostatic potential (ESP) is a rigorously defined, real physical property that can be calculated directly from the charge distribution or molecular wave function.<sup>1-3</sup> In terms of the wave function, the ESP at the point  $r$  is defined as:

$$V(r) = \sum_A \frac{Z_A}{|R_A - r|} - \int \frac{\psi^*(r')\psi(r') dr'}{|r' - r|} \quad (1)$$

It is now well-recognized<sup>4-12</sup> that electrostatic potentials play an important role in the analysis, and understanding of long range noncovalent interactions such as hydrogen bonding, solvation, crystal packing, and protein-ligand interactions, and especially in the definition of electrostatic potential-derived atomic charges. Because these charges may be interpreted as the atom-centered monopole approximation to the molecular charge density, they represent one of the most unambiguous and rigorous definitions of atomic charge, and have generally been considered to be highly suitable for describing the long-range coulombic interactions in molecular force fields.

Whereas the calculation of electrostatic-potential-derived atomic charges for small molecules is simple, it is quite computationally intensive for large systems. A three-step process is required. First, the wave function must be computed. Second, the ESP is calculated from the wave function for a large number of points in the region outside the van der Waals envelope of the molecule (where the monopole approximation to the charge density is valid). Third, a set of least squares equations is solved which defines the atomic charges that best reproduce the quantum-mechanically derived ESPs subject to various constraints. Charges derived from *ab initio* Hartree-Fock 6-31G\* calculations are generally accepted as being sufficiently accurate, even though it is clear that Hartree-Fock wave functions are in general too ionic. Even at this level of theory, the calculation of wave functions for typical molecules of biological interest, with 50 or more atoms, is not a trivial task. For this reason, a significant amount of work has appeared on the application of semiempirical methods to this problem. A detailed discussion of the accuracy of various semiempirical methods for the calculation of ESP-derived charges may be found in the first part of this series.<sup>13</sup> However, it should be

noted that AM1, MNDO, and PM3 ESP-derived atomic charges exhibit systematic errors when compared with HF/6-31G\* values, and require large scaling factors (1.25-1.5) to bring the charges into reasonable agreement with the *ab initio* values. Even with scaling factors, these methods typically produce average absolute errors in the range of 0.07-0.10e<sup>-</sup> compared with HF/6-31G\* calculations.<sup>14,15</sup> Furthermore, the best scaling factor may depend on the nature of the molecule. For instance, Merz<sup>15</sup> examined a large data set of amino acids and monosaccharides containing 1007 atoms. He compared charges derived from HF/6-31G\* calculations and various semiempirical approaches. He found much better agreement with MNDO wave functions ( $r = 0.96$ ) than AM1 ( $r = 0.81$ ) or PM3 ( $r = 0.70$ ), but even the MNDO charges required a large scaling factor (1.29) to obtain optimum agreement with the *ab initio* values. He also demonstrated that the best scaling factor for MNDO charges is significantly different for amino acids (1.26) than for monosaccharides (1.47).

Most semiempirical approaches to the calculation of ESP-derived atomic charges suffer from another problem: they require analytical evaluation of the electrostatic potential, a process that easily dominates the cpu time requirements of the entire procedure. An encouraging approach to circumventing this problem was recently proposed by Wang and Ford (WF).<sup>16,17</sup> In this approach, the molecular electrostatic potential is not calculated analytically, but is evaluated via new semiempirical expressions that involve only two-center terms. This approach is approximately two orders of magnitude faster than methods that employ semiempirical wave functions and analytic evaluation of the electrostatic potential, while achieving reasonable accuracy in both the high and low potential regions surrounding the molecule. For a collection of 21 molecules containing H, C, N, and O atoms, WF found an average absolute error (relative to HF 6-31G\*) of 0.097e and a correlation coefficient of 0.963. When a uniform scaling factor of 1.208 was applied to the calculated charges, the error was reduced to 0.073e. A second, very recent approach to the rapid calculation of ESP-derived atomic charges at the semiempirical level is the VESPA method of Beck, et al.<sup>18</sup> In this approach, the ESP is evaluated directly from a semiempirical wave function, but the charge distribution of each heavy atom is represented by nine point charges (one of which is atom-centered) and the charge distribution of each hydrogen is represented by a

single point charge. The ESP calculation is therefore reduced to a trivial double sum that is extremely fast. For 26 molecules containing H, C, O, N, S, and P, VESPA yielded the best results (relative to HF/6-31G\* calculations) with AM1 wave functions, where the overall correlation coefficient was 0.934 and the average absolute deviation (not reported by them, but calculated here on the basis of their published data) was  $0.096e^-$ . Thus, both of these semiempirical methods represent very efficient approaches to the calculation of ESP-derived charges, although they still suffer from significant inaccuracies likely to make them unacceptable for calculation of high-quality, long-range electrostatics. In addition, neither of these methods have been evaluated for their ability to reproduce atomic charges from correlated wave functions. The importance of electron correlation has been made apparent in a recent study by Wampler,<sup>19</sup> who showed that electron correlation accounts for about a 10% change in the ESP-derived charges. This is not a trivial effect, because ESP-derived charges are often quite large.

In part I of this series,<sup>13</sup> a new approach for the calculation of ESP-derived charges was presented. Denoted *PESP* (Parameterized ElectroStatic Potential), this method is based on modified PRDDO/M wave functions<sup>20–25</sup> and parameterized against correlated wave functions employing the 6-31G\*\* basis set. Intermediate in computational complexity between a fully *ab initio* and a fully semiempirical approach, *PESP* is an order of magnitude faster than the simplest *ab initio* approach (STO-3G), while achieving a degree of accuracy approaching that of the reference calculations which it is parameterized against (*ab initio* MP2/6-31G\*\*). Unlike previous approximate methods, *PESP* achieves high accuracy through a direct parameterization of the wave function and analytic (but rapid) calculation of the resultant electrostatic potentials. Part I of this series described the *PESP* parameterization for organic and inorganic species containing H, C, N, O, F, P, S, Cl, and Br, including hypervalent species for P, S, and Cl. In addition, the algorithm for the rapid near-analytic evaluation of the ESP over Slater orbitals was described. An overall unscaled average absolute deviation relative to MP2/6-31G\*\* values of  $0.037e^-$  for 820 symmetry unique atoms in 145 molecules was achieved, with a correlation coefficient of 0.990. In part II, this approach was extended<sup>26</sup> to the calculation of molecular electrostatic potentials in the high potential regions (inside the molecular van der Waals envelope). It was

shown that simple modifications of the *PESP* procedure result in highly accurate representations of the ESP inside the van der Waals envelope. For instance, the location and depth of lone-pair minima can be calculated with an average error (relative to MP2/6-31G\*\*) of 0.03 Å and 2.5 kcal/mol, respectively. Furthermore, *PESP* maps of the molecular electrostatic potential are sometimes nearly indistinguishable from their MP2/6-31G\*\* counterparts.

Although the *PESP* method represents a significant advancement in accuracy (relative to semiempirical approaches) and in computational speed (relative to *ab initio* methods) it still is not applicable to a broad enough range of elements to be useful as a general tool for the exploration of biomolecular electrostatics. In particular, to be useful for protein electrostatics, *PESP* must be able to calculate high-quality electrostatics for species containing a variety of metal ions. In this study, the *PESP* method is extended to molecules containing  $Li^+$ ,  $Na^+$ ,  $Mg^{2+}$ ,  $K^+$ ,  $Ca^{2+}$ ,  $Zn^{2+}$ , and I. For a collection of 166 molecules containing 1668 atoms with at least one metal or iodine atom, *PESP* achieves (without scaling) an average absolute deviation in ESP-derived charges of  $0.042e^-$  compared with *ab initio* MP2/6-31G\*\* values, with a correlation coefficient of 0.996. For a larger data set consisting of 311 molecules, taken from part I and the current work, and encompassing all 16 elements just listed (2488 total atoms), *PESP* reproduces the *ab initio* ESP-derived charges with an overall average unscaled absolute deviation of  $0.040e^-$  and a correlation coefficient of 0.995.

---

## PRDDO/M and PESP Methods

A full description of the PRDDO/M method may be found in the original references.<sup>20–25</sup> PRDDO/M is an approximate molecular orbital approach designed to reproduce *ab initio* minimum basis set calculations with a Slater orbital basis set at a fraction of the computational cost. Because it is parameterized against *ab initio* calculations and not experiment, PRDDO/M may be regarded as a nonempirical approach. The essence of the PRDDO/M method may be summarized as follows. First, almost all one-, two-, and three-center integrals are calculated explicitly to at least three-decimal-place accuracy. Second, the integrals are transformed to a Löwdin<sup>27</sup> orthogonalized basis. In this basis, four-function two-electron inte-

grals of the form  $(ij|kl)$  are small and may be neglected without significant loss of accuracy. This reduces the formal computational dependence of the method from  $n^4$  to  $n^3$ . However, for computational efficiency, the transformation from the atomic orbital basis to the Löwdin basis is not done exactly: certain nonzero (but small) terms are neglected. This requires the introduction of a small set (four or five per atom) of parameters, which are derived by comparison to *ab initio* calculations, to correct the results to the full *ab initio* values. Unlike semiempirical methods, PRDDO/M is only weakly parameterized. Elimination of all parameters still results in reasonable molecular properties when compared with the reference *ab initio* results. Indeed, PRDDO/M currently contains no parameters for the first transition metal series, but has been used quite successfully to describe structure and bonding in a wide range of transition metal complexes.<sup>28</sup>

The essence of the *PESP* modifications to the PRDDO/M method is extremely simple. A *PESP* calculation is simply a PRDDO/M/FCP (frozen-core potential) calculation with a new set of parameters chosen to minimize an error function based on ESP-derived atomic charges:

$$\varepsilon = \sum_i |q_i^{ab\text{ initio}} - q_i^{PESP}| \quad (2)$$

For the elements in part I, the parameters consisted of the orbital exponents and two additional variables, which modified (in a multiplicative fashion) two-center integrals of the form  $(\chi_{1sH} \chi_{jA} | \chi_{jA}^2)$  and one-center integrals of the form  $(\chi_{jA}^2 | \chi_{jA}^2)$ , where  $j$  runs over a set of valence  $s$  and  $p$  orbitals. In this article, a similar treatment was used for iodine, where only the orbital exponents were taken as free parameters. For the metals, however, it was found that varying only the orbital exponents did not yield satisfactory results, and that modifications of the above mentioned two-electron integrals were ineffective in minimizing the error function. Therefore, a new set of parameters had to be developed.

Metal systems, even as simple as alkali metal complexes, proved to be a challenge for effective parameterization. The basic problem is easily understood: PRDDO/M, like any *ab initio* or near *ab initio* minimum basis set method, overestimates the importance of the valence  $s$  and  $p$  orbitals on the metal, and thus exaggerates metal–ligand covalent bonding. Parameterizations that include only the orbital exponents compensate for this

effect by contracting the valence  $s$ – $p$  shell. However, this results in a metal ion with a far-too-high charge:radius ratio, which in turn produces exaggerated polarization effects on the ligands. After considerable experimentation, it was found that this problem could be dealt with by parameterizing two center nuclear attraction integrals of the form  $(\chi_{iA}^2 \chi_{jA}^2 | 1/R_{1B})$ . Here  $B$  is a metal center, and  $i$  and  $j$  run over the valence  $s$  and  $p$  orbitals of atom  $A$ . Details of the computational procedures are discussed next.

## Computational Details

For each atom, a reference parameterization set (RPS) of molecules was generated (Tables I–VII). Geometries for these molecules were obtained from Hartree–Fock-level optimizations. Geometry optimizations were performed on an IBM RS-6000 Model 250 computer using the program GAMESS.<sup>29</sup> Most optimizations were performed at the 6-31G\* (6d) level<sup>30</sup> or SBK<sup>31</sup> (with NDFUNC = 1) as defined in GAMESS; however, some molecules were optimized at the 3-21G level<sup>32</sup> in an effort to make the parameterization largely independent of the theoretical model used to obtain the geometry. To make the *ab initio* calculations tractable, simple ligands had to be employed in all of the metal complexes. This also had the advantage of keeping the metal ion from being too buried in the molecular interior to have well-defined atomic charges (see subsequent text). The ligands employed included H<sub>2</sub>O, H<sub>3</sub>N, H<sub>3</sub>P, H<sub>2</sub>S, CO, the formate anion, formaldehyde, pyridine, OH<sup>−</sup>, HF, HCl, and HBr (the latter three as models of alkylhalide systems). A range of coordination numbers, appropriate for each metal, was included.

All *ab initio* ESP-derived charges were obtained at the MP2/6-31G\*\* level using Gaussian-94<sup>33</sup> on an NEC SX-4 computer. For all atoms except Zn, K, Ca, and I, the standard 6-31G\*\* basis set<sup>30</sup> was used. For K and Ca, the TZV basis set of Schafer, et al.<sup>34</sup> was employed, supplemented with one additional  $p$  and  $d$  function (exponents = 0.10). The same style basis set was used for Zn, except that it was supplemented by two  $p$  functions, with exponents of 0.1430 and 0.0508. For iodine, the SBKJC<sup>35</sup> basis set was used, with an additional  $d$  function having an exponent of 0.266. The assumed symmetries and the basis set employed for the geometry optimizations of each molecule are listed in Tables I–VII.

TABLE I.  
Molecules in Lithium RPS.<sup>a, b</sup>

$\text{Li}(\text{NH}_3)_3(\text{OCH}_2)^+$	$\text{Li}(\text{NH}_3)_3(\text{Py})^{+ \text{ c}}$	$\text{Li}(\text{NH}_3)_4^+$	$\text{Li}(\text{H}_2\text{O})_2(\text{NH}_3)_2^+$
$\text{Li}(\text{H}_2\text{O})_2(\text{NH}_3)_4^+$	$\text{Li}(\text{H}_2\text{O})_2(\text{ClH})_2^+$	$\text{Li}(\text{H}_2\text{O})_2(\text{PH}_3)_2^+$	$\text{Li}(\text{H}_2\text{O})_2(\text{SH}_2)_2^+$
$\text{Li}(\text{H}_2\text{O})(\text{NH}_3)_3^+$	$\text{Li}(\text{H}_2\text{O})_3(\text{HCO}_2)^+$	$\text{Li}(\text{H}_2\text{O})_3(\text{ClH})^+$	$\text{Li}(\text{H}_2\text{O})_3(\text{FH})^+$
$\text{Li}(\text{H}_2\text{O})_3(\text{SH}_2)^+$	$\text{Li}(\text{H}_2\text{O})_4^+$	$\text{Li}(\text{H}_2\text{O})_4(\text{Py})^{+ \text{ d}}$	$\text{Li}(\text{H}_2\text{O})_5(\text{NH}_3)^{+ \text{ c}}$
$\text{Li}(\text{H}_2\text{O})_5(\text{ClH})^{+ \text{ c}}$	$\text{Li}(\text{H}_2\text{O})_5(\text{FH})^{+ \text{ c}}$	$\text{Li}(\text{H}_2\text{O})_5(\text{PH}_3)^{+ \text{ c}}$	

<sup>a</sup> Optimized at the HF/6-3 1G\* level unless otherwise indicated.  
<sup>b</sup> All molecules are C<sub>s</sub> symmetry unless otherwise indicated.  
<sup>c</sup> Geometry calculated at the HF/3-21G level.  
<sup>d</sup> C<sub>2v</sub> symmetry.

TABLE II.  
Molecules in Sodium RPS.<sup>a, b</sup>

$\text{Na}(\text{NH}_3)_3(\text{Py})^{+ \text{ c}}$	$\text{Na}(\text{NH}_3)_4^+$	$\text{Na}(\text{NH}_3)(\text{H}_2\text{O})_5^+$	$\text{Na}(\text{H}_2\text{O})_2(\text{HCO}_2)$
$\text{Na}(\text{H}_2\text{O})_3(\text{NH}_3)^{+ \text{ c}}$	$\text{Na}(\text{H}_2\text{O})_3(\text{ClH})^+$	$\text{Na}(\text{H}_2\text{O})_3(\text{FH})^+$	$\text{Na}(\text{H}_2\text{O})_3(\text{PH}_3)^+$
$\text{Na}(\text{H}_2\text{O})_3(\text{SH}_2)^+$	$\text{Na}(\text{H}_2\text{O})_4^+$	$\text{Na}(\text{H}_2\text{O})_4(\text{PH}_3)_2^{+ \text{ c}}$	$\text{Na}(\text{H}_2\text{O})_4(\text{SH}_2)_2^{+ \text{ c}}$
$\text{Na}(\text{H}_2\text{O})_5(\text{ClH})^{+ \text{ c}}$	$\text{Na}(\text{H}_2\text{O})_5(\text{ClH})^{+ \text{ c}}$	$\text{Na}(\text{H}_2\text{O})_5(\text{FH})^{+ \text{ c}}$	$\text{Na}(\text{H}_2\text{O})_5(\text{FH})^{+ \text{ d, e}}$
$\text{Na}(\text{H}_2\text{O})_5(\text{PH}_3)^{+ \text{ c}}$	$\text{Na}(\text{H}_2\text{O})_5(\text{Py})^{+ \text{ e}}$	$\text{Na}(\text{H}_2\text{O})_6^{+ \text{ f}}$	

<sup>a</sup> Optimized at the HF/6-31G\* level unless otherwise indicated.  
<sup>b</sup> All molecules are C<sub>s</sub> symmetry unless otherwise indicated.  
<sup>c</sup> Geometry calculated at the HF/3-21G level.  
<sup>d</sup> Geometry calculated at the HF/SBK + d level (see text).  
<sup>e</sup> C<sub>2v</sub> symmetry.  
<sup>f</sup> D<sub>2h</sub> symmetry.

TABLE III.  
Molecules in Magnesium RPS.<sup>a, b</sup>

$\text{Mg}(\text{NH}_3)_3(\text{OCH}_2)^{2+}$	$\text{Mg}(\text{NH}_3)_3(\text{Py})^{2+ \text{ c}}$	$\text{Mg}(\text{NH}_3)_4^{2+}$	$\text{Mg}(\text{NH}_3)(\text{H}_2\text{O})_5^{2+}$
$\text{Mg}(\text{PH}_3)_4^{2+}$	$\text{Mg}(\text{SH}_2)_2(\text{ClH})_2^{2+}$	$\text{Mg}(\text{SH}_2)_4^{2+}$	$\text{Mg}(\text{H}_2\text{O})_2(\text{ClH})_2^{2+}$
$\text{Mg}(\text{H}_2\text{O})_2(\text{FH})_2^{2+}$	$\text{Mg}(\text{H}_2\text{O})_2(\text{FH})(\text{ClH})^{2+}$	$\text{Mg}(\text{H}_2\text{O})_4^{2+}$	$\text{Mg}(\text{H}_2\text{O})_4(\text{PH}_3)_2^{2+}$
$\text{Mg}(\text{H}_2\text{O})_3\text{Cl}^+$	$\text{Mg}(\text{H}_2\text{O})_3(\text{ClH})^{2+}$	$\text{Mg}(\text{H}_2\text{O})_3(\text{FH})^{2+}$	$\text{Mg}(\text{H}_2\text{O})_3(\text{HCO}_2)^+$
$\text{Mg}(\text{H}_2\text{O})_3(\text{PH}_3)^{2+}$	$\text{Mg}(\text{H}_2\text{O})_3(\text{SH}_2)^{2+}$	$\text{Mg}(\text{H}_2\text{O})_4(\text{NH}_3)_2^{2+}$	$\text{Mg}(\text{H}_2\text{O})_3(\text{NH}_3)^{2+}$
$\text{Mg}(\text{H}_2\text{O})_6^{2+ \text{ e}}$	$\text{Mg}(\text{H}_2\text{O})_4(\text{FH})(\text{ClH})^{2+}$	$\text{Mg}(\text{H}_2\text{O})_5(\text{ClH})^{2+ \text{ c}}$	$\text{Mg}(\text{H}_2\text{O})_5(\text{FH})^{2+ \text{ c}}$
$\text{Mg}(\text{H}_2\text{O})_5(\text{PH}_3)^{2+}$	$\text{Mg}(\text{H}_2\text{O})_5(\text{PY})^{2+ \text{ c, d}}$	$\text{Mg}(\text{H}_2\text{O})_5(\text{SH}_2)^{2+ \text{ c, d}}$	$\text{Mg}(\text{H}_2\text{O})_2(\text{SH}_2)(\text{PH}_3)^{2+}$

<sup>a</sup> Optimized at the HF/6-31G\* level unless otherwise indicated.  
<sup>b</sup> All molecules are C<sub>s</sub> symmetry unless otherwise indicated.  
<sup>c</sup> Geometry calculated at the HF/3-21G level.  
<sup>d</sup> C<sub>2v</sub> symmetry.  
<sup>e</sup> D<sub>2h</sub> symmetry.

TABLE IV.  
Molecules in Potassium RPS.<sup>a, b</sup>

$\text{K}(\text{NH}_3)_5(\text{OH})$	$\text{K}(\text{H}_2\text{O})_2(\text{SH}_2)_2^+$	$\text{K}(\text{H}_2\text{O})_3(\text{ClH})^+$	$\text{K}(\text{H}_2\text{O})(\text{PH}_3)_3^+$
$\text{K}(\text{H}_2\text{O})_3(\text{PH}_3)_2^+$	$\text{K}(\text{H}_2\text{O})_4(\text{NH}_3)_2^+$	$\text{K}(\text{H}_2\text{O})(\text{PH}_3)_4^+$	$\text{K}(\text{H}_2\text{O})_4(\text{PH}_3)_2^{+ \text{ c}}$
$\text{K}(\text{H}_2\text{O})(\text{SH}_2)_4^{+ \text{ d}}$	$\text{K}(\text{H}_2\text{O})_5^{+ \text{ d}}$	$\text{K}(\text{H}_2\text{O})_5(\text{ClH})^{+ \text{ d}}$	$\text{K}(\text{H}_2\text{O})_5(\text{FH})^{+ \text{ d}}$
$\text{K}(\text{H}_2\text{O})_5(\text{HCO}_2)^{\text{d}}$	$\text{K}(\text{H}_2\text{O})_5(\text{OCH}_2)^{+ \text{ d}}$	$\text{K}(\text{H}_2\text{O})_5(\text{OH})^{\text{f}}$	$\text{K}(\text{H}_2\text{O})_5(\text{OH})^{\text{f}}$
$\text{K}(\text{H}_2\text{O})_5(\text{PH}_3)^{+ \text{ c}}$	$\text{K}(\text{H}_2\text{O})_5(\text{Py})^{+ \text{ d}}$	$\text{K}(\text{H}_2\text{O})_5(\text{SH}_2)^{+ \text{ c}}$	$\text{K}(\text{H}_2\text{O})_6(\text{NH}_3)^{+ \text{ g}}$
$\text{K}(\text{H}_2\text{O})_7^+$	$\text{K}(\text{H}_2\text{O})_8^{+ \text{ g}}$		

<sup>a</sup> Optimized at the HF/SBK + d level unless otherwise indicated (see text).  
<sup>b</sup> All molecules are C<sub>s</sub> symmetry unless otherwise indicated.  
<sup>c</sup> Geometry calculated at the HF/3-21G level.  
<sup>d</sup> C<sub>2v</sub> symmetry.  
<sup>e</sup> D<sub>2h</sub> symmetry.  
<sup>f</sup> Two different structures with C<sub>s</sub> symmetry were located for this species.  
<sup>g</sup> C<sub>1</sub> symmetry.

**TABLE V.**  
**Molecules in Calcium RPS.<sup>a, b</sup>**

$\text{Ca}(\text{NH}_3)_4^{2+}$	$\text{Ca}(\text{NH}_3)_6^{2+}$	$\text{Ca}(\text{H}_2\text{O})_3(\text{ClH})_2^{2+}$	$\text{Ca}(\text{H}_2\text{O})_3(\text{HCO}_2)^+$
$\text{Ca}(\text{H}_2\text{O})_3(\text{PH}_3)^{2+}$	$\text{Ca}(\text{H}_2\text{O})_4^{2+}$	$\text{Ca}(\text{H}_2\text{O})_4(\text{NH}_3)^{2+}$	$\text{Ca}(\text{H}_2\text{O})_4(\text{ClH})_2^{2+}$
$\text{Ca}(\text{H}_2\text{O})_4(\text{SH}_2)_2^{2+}$	$\text{Ca}(\text{H}_2\text{O})_5^{2+}$	$\text{Ca}(\text{H}_2\text{O})_5(\text{NH}_3)^{2+}$	$\text{Ca}(\text{H}_2\text{O})_5(\text{ClH})^{2+ c}$
$\text{Ca}(\text{H}_2\text{O})_5(\text{FH})^{2+ c}$	$\text{Ca}(\text{H}_2\text{O})_5(\text{HCO}_2)^+ c$	$\text{Ca}(\text{H}_2\text{O})_5(\text{OCH}_2)^{2+ c}$	$\text{Ca}(\text{H}_2\text{O})_5(\text{OH})^+$
$\text{Ca}(\text{H}_2\text{O})_5(\text{PH}_3)^{2+}$	$\text{Ca}(\text{H}_2\text{O})_5(\text{Py})^{2+ c}$	$\text{Ca}(\text{H}_2\text{O})_5(\text{SH}_2)^{2+ c}$	$\text{Ca}(\text{H}_2\text{O})_6^{2+ d}$

<sup>a</sup> Optimized at the HF/SBK + d level (see text).

<sup>b</sup> All molecules are  $C_s$  symmetry unless otherwise indicated.

<sup>c</sup>  $C_{2v}$  symmetry.

<sup>d</sup>  $D_{2h}$  symmetry.

**TABLE VI.**  
**Molecules in Zinc RPS.<sup>a, b</sup>**

$\text{Zn}(\text{NH}_3)_2(\text{CH}_3)_2$	$\text{Zn}(\text{NH}_3)_2(\text{H}_2\text{O})_2^{2+}$	$\text{Zn}(\text{NH}_3)_3(\text{CH}_3)^+$	$\text{Zn}(\text{NH}_3)_2(\text{H}_2\text{O})(\text{SH}_2)^{2+ d}$
$\text{Zn}(\text{NH}_3)_3(\text{OH})^+$	$\text{Zn}(\text{NH}_3)_3(\text{H}_2\text{O})^{2+}$	$\text{Zn}(\text{NH}_3)_4^{2+}$	$\text{Zn}(\text{NH}_3)_4(\text{OH})^+$
$\text{Zn}(\text{NH}_3)_3(\text{H}_2\text{O})_2^{2+}$	$\text{Zn}(\text{CO})(\text{H}_2\text{O})_2\text{Cl}^+$	$\text{Zn}(\text{CO})_4^{2+ c}$	$\text{Zn}(\text{H}_2\text{O})_3\text{Cl}^+$
$\text{Zn}(\text{H}_2\text{O})_3(\text{FH})^{2+}$	$\text{Zn}(\text{H}_2\text{O})_3(\text{HCO}_2)^+$	$\text{Zn}(\text{H}_2\text{O})_3(\text{SH}_2)_2^{2+ c}$	$\text{Zn}(\text{H}_2\text{O})_3(\text{BrH})^{2+}$
$\text{Zn}(\text{H}_2\text{O})_3(\text{ClH})^{2+}$	$\text{Zn}(\text{H}_2\text{O})_3(\text{PH}_3)^{2+}$	$\text{Zn}(\text{H}_2\text{O})_4^{2+}$	$\text{Zn}(\text{H}_2\text{O})_4(\text{NH}_3)^{2+}$
$\text{Zn}(\text{H}_2\text{O})_4(\text{NH}_3)_2^{2+}$	$\text{Zn}(\text{H}_2\text{O})_4(\text{PH}_3)_2^{2+}$	$\text{Zn}(\text{H}_2\text{O})_4(\text{SH}_2)^{2+ c}$	$\text{Zn}(\text{H}_2\text{O})_4(\text{SH}_2)^{2+ c}$
$\text{Zn}(\text{H}_2\text{O})_5(\text{NH}_3)^{2+}$	$\text{Zn}(\text{H}_2\text{O})_5\text{Cl}^+ c$	$\text{Zn}(\text{H}_2\text{O})_5(\text{ClH})^{2+ c}$	$\text{Zn}(\text{H}_2\text{O})_5(\text{FH})^{2+ c}$
$\text{Zn}(\text{H}_2\text{O})_5(\text{BrH})^{2+ c}$	$\text{Zn}(\text{H}_2\text{O})_5(\text{OCH}_2)^{2+ c}$	$\text{Zn}(\text{H}_2\text{O})_5(\text{Py})^{2+ c}$	$\text{Zn}(\text{H}_2\text{O})_6^{2+}$

<sup>a</sup> Optimized at the HF/SBK + d level.

<sup>b</sup> All molecules are  $C_s$  symmetry unless otherwise indicated.

<sup>c</sup>  $C_{2v}$  symmetry.

<sup>d</sup>  $C_1$  symmetry.

<sup>e</sup>  $T_d$  symmetry.

**TABLE VII.**  
**Molecules in Iodine RPS.<sup>a</sup>**

1,2-Bromoiodoethylene	$\text{CH}_3\text{I}$	$\text{Cl}_3\text{COOH}$	$\text{Cl}_3\text{H}$
$\text{Cl}_4$	$\text{H}_2\text{ClCl}$	1,1-Chloroiodoethylene	$\text{C}(\text{CH}_3)_2\text{I}(\text{OH})$
1,1-Fluoroiodoethylene	$\text{HC}(\text{CH}_3)_2\text{I}$	$\text{HCOI}$	$\text{HI}$
1,1-Diiodoethylene	$\text{HOI}$	Iodobenzene	$\text{CBrI}_2$
Iodoacetylene	$\text{ICN}$	2-Iodofuran	<i>p</i> -Iodopyridine
$\text{NH}_2\text{I}$	$\text{OI}_2$	$\text{PH}_2\text{I}$	$\text{ISH}$
1,2-Bromoiodoethane	Bromoiodoacetylene		

<sup>a</sup> Optimized at the HF/SBK + d level (see text).

The ESP-derived charges at both the *ab initio* and the *PESP* levels were calculated using the Merz–Kollman algorithm.<sup>14, 36–38</sup> This method calculates the ESP at a set of points distributed on atom-centered spheres with radii that are some multiples (typically 1.4, 1.6, 1.8, and 2.0) of the van der Waals radius of the atom. Because recommended van der Waals radii for the Merz–Kollman algorithm appear not to be available for K, Ca, and I, they were determined in this work. Although it is possible to estimate appropriate radii based on literature values or periodic trends, a more practical approach was taken here. For

$\text{K}(\text{H}_2\text{O})_4(\text{NH}_3)_2^+$ ,  $\text{K}(\text{H}_2\text{O})_6^+$ ,  $\text{Ca}(\text{H}_2\text{O})_4(\text{NH}_3)_2^{2+}$ ,  $\text{Ca}(\text{H}_2\text{O})_6^{2+}$ ,  $\text{CH}_3\text{I}$ ,  $\text{H}(\text{CO})\text{I}$ ,  $\text{OI}_2$ , and iodobenzene, the *ab initio* ESP-derived atomic charges were determined as a function of the assumed van der Waals radius. A radius was then selected for each atom from plots of the calculated charge for the atom in question versus the assumed van der Waals radius. These plots are shown in Figure 1 for potassium and calcium and in Figure 2 for iodine. The radius chosen, indicated by a vertical line, corresponds approximately to the value for which the calculated charge is least sensitive to the assumed radius. For potassium and calcium, any

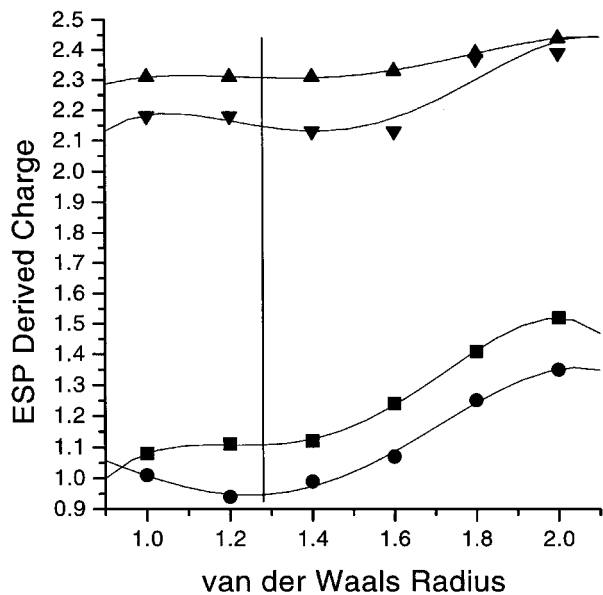


**FIGURE 1.** Plot of ESP-derived charges for  $\text{K}(\text{H}_2\text{O})_4(\text{NH}_3)_2^+$  (circles),  $\text{K}(\text{H}_2\text{O})_6^+$  (squares),  $\text{Ca}(\text{H}_2\text{O})_4(\text{NH}_3)_2^{2+}$  (triangles), and  $\text{Ca}(\text{H}_2\text{O})_6^{2+}$  (inverted triangles) as a function of assumed van der Waals radius. The vertical line indicates the radius chosen (see text).

value in the range of 1.0–1.4 Å is acceptable, but, for simplicity, a common value of 1.24 Å was chosen. For iodine, the calculated charges are quite insensitive to the assumed radius over a wide range, and a value of 2.5 Å was chosen. All of these calculations were done at the Hartree–Fock level, with the standard GAMESS TZV + d basis set<sup>39</sup> for potassium- and calcium-containing molecules and the SBK + d basis set for the molecules containing iodine.<sup>40</sup>

PRDDO/M (and, therefore, *PESP*) is currently available only for the elements H–Ar and Sc–Kr.

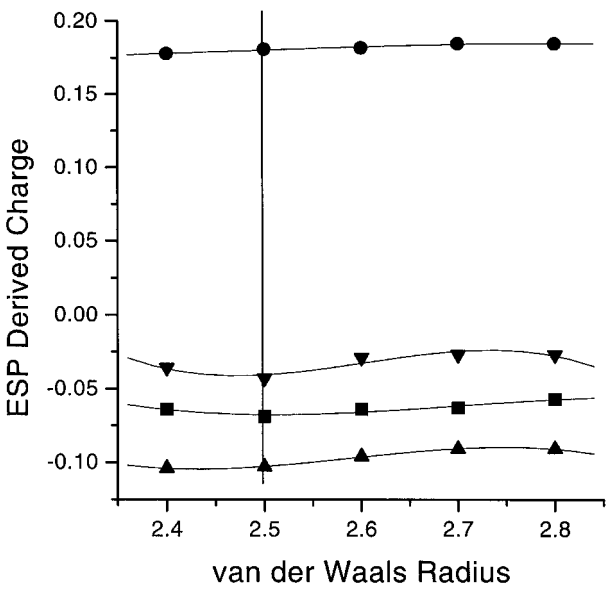


**FIGURE 2.** Plot of ESP-derived charges for  $\text{CH}_3\text{I}$  (squares), iodobenzene (inverted triangles),  $\text{H}(\text{CO})\text{I}$  (triangles),  $\text{OI}_2$  (circles) as a function of assumed van der Waals radius. The vertical line indicates the radius chosen (see text).

The elements K and Ca are not implemented in the method, because their unique orbital structure in the minimum basis set approximation,  $1s2sp3sp4sp$  (as opposed to  $1s2sp3sp3d4sp$  for the remainder of the fourth row elements), has not yet been programmed. Similarly, PRDDO/M calculations on iodine are not yet possible, because analytic two-center coulomb integrals have been programmed only through  $n = 4$ . However, it is still possible to generate *PESP* parameters for K, Ca, and I. *PESP* is a valence-electron-only method, and uses frozen-core potentials (constructed from

**TABLE VIIIA.**  
**Optimized Parameters.**

	Nuclear attraction parameters							
	N–F				P–Cl			
	P	$C_{ss}$	$C_{sp}$	$C_{pp}$	P	$C_{ss}$	$C_{sp}$	$C_{pp}$
Li	3.000 <sup>a</sup>	2.341	–8.758	0.824	—	—	—	—
Na	4.080	3.418	–1.418	2.010	—	—	—	—
Mg	4.682	2.839	–9.281	0.753	3.000 <sup>a</sup>	—	10.905	—
K	3.000 <sup>a</sup>	2.310	—	= <sup>b</sup>	—	—	—	—
Ca	2.992	1.949	–0.241	1.174	—	—	—	—
Zn	5.864	2.421	–3.531	0.993	—	—	—	—

<sup>a</sup> Constrained (see text).  
<sup>b</sup>  $C_{sp} = C_{ss}$ .

**TABLE VIII.B.**  
**Optimized Parameters.**

	Exponents				
	1s	2sp	3sp	4sp	3d
Li	2.487	1.896	—	—	—
Na	U <sup>a</sup>	2.338	2.752	—	—
Mg	U <sup>a</sup>	2.894	2.832	—	—
K <sup>b</sup>	U <sup>a</sup>	3.717	1.757	—	—
Ca <sup>c</sup>	U <sup>a</sup>	5.668	1.788	—	—
Zn	17.076	U <sup>a</sup>	U <sup>a</sup>	3.543	3.748
I <sup>d</sup>	5.726	10.220	8.093	2.692	U <sup>a</sup>

<sup>a</sup> Unmodified.

<sup>b</sup> Treated as pseudo-Na atom (see text).

<sup>c</sup> Treated as pseudo-Mg atom (see text).

<sup>d</sup> Treated as pseudo-Br atom (see text).

the core orbital electron repulsion integrals and containing the appropriate projection operators<sup>23–24</sup>). Thus, in the frozen-core approximation, potassium can be treated as sodium, calcium as magnesium, and iodine as bromine, simply by substituting a different core potential and a rescaled valence shell exponent. Because the core potential is derived from the electron repulsion integrals and the orbital exponents are taken as free parameters in the electrostatic potential fits, the appropriate core potentials and valence shell exponent are found automatically during the minimization of the error function. This procedure works extremely well (see subsequent text).

The parametric form for a *s*–*s* nuclear attraction integral is:

$$\left( S_A S_B \left| \frac{1}{R_{AB}} \right. \right)_{PARA} = \left( S_A S_B \left| \frac{1}{R_{AB}} \right. \right)_{EXACT} \cdot (1 + C_{ss} P^{(r-crada)}) \quad (3)$$

where *crad<sub>A</sub>* is the covalent radius of atom *A*, *r* is the internuclear distance, and atom *B* is a metal center. This correction was applied to all nonzero components of the integrals in a local diatomic coordinate system, before rotation to the general coordinate system. For *s*–*p* and *p*–*p* components, a common value of *P* was used, and only one additional parameter per integral (*C<sub>sp</sub>* and *C<sub>pp</sub>*) was introduced. In all elements, except magnesium, parameterization was restricted to M–N, M–O, and M–F interactions and, in some cases, the parameter *C<sub>mn</sub>* (*m, n* = *s* or *p*) in eq. (3) was set to zero if the parameter did not strongly affect the calculated error function. Parameter *P* was never allowed to take on a value of less than 3.0.

This insures the correct long-range behavior of the modified nuclear attraction terms. (An exception is Ca, for which the optimized value for *P* of 2.992 was employed.)

Only the charges of symmetry-unique atoms were considered, and the parameters previously determined<sup>13</sup> for H, C, N, O, F, P, S, Cl, and Br were used without change. A simplex procedure was used for optimization of the parameters.

## Results and Discussion

The number of molecules in the *ab initio* RPS depended in part on the number of independent parameters optimized, and varied from 19 (Li) to 32 (Zn). The final parameters are reported in Table VII, and the statistical results are summarized in Tables IX–XV. For each element in each data set, the number of atoms, the average absolute charge at the MP2/6-31G\*\* level, the average absolute deviation and the average signed deviation are tabulated. In addition, the overall average deviation for each data set is reported, as is the correlation coefficient and the linear least-squares parameters **m** and **b** (taking the *ab initio* values as the dependent variable).

The results for the metal complexes may be discussed as a group, because the general behavior of the method is similar for all metal ions. Hydrogen charges are very accurately determined, with the largest average absolute deviation being only 0.026e<sup>–</sup> (Zn) and the smallest being 0.016e<sup>–</sup> (Ca). This was also true for the molecules from part I (where an average absolute deviation of 0.019e<sup>–</sup> was found) and is a reflection of the fact that



**TABLE IX.**  
**Statistical Results for Lithium RPS.**

Atom	Number	Avg. abs. charge	Avg. abs. deviation	Avg. signed deviation
H	115	.376	.024	.000
Li	19	.847	.090	−.003
C	10	.185	.049	−.027
N	16	.934	.079	−.008
O	41	.913	.052	.022
F	2	.514	.022	−.022
P	3	.111	.179	−.179
S	3	.402	.035	−.015
Cl	3	.295	.019	.007
All	212		.043	

No. of molecules = 19;  $r = 0.994$ ;  $m = 1.008$ ;  $b = 0.001$ .

**TABLE X.**  
**Statistical Results for Sodium RPS.**

Atom	Number	Avg. abs. charge	Avg. abs. deviation	Avg. signed deviation
H	119	.385	.023	.003
C	9	.187	.041	.002
N	9	.856	.052	−.033
O	51	.923	.042	.003
F	3	.532	.041	.011
Na	19	.939	.061	−.001
P	4	.229	.101	−.101
S	3	.449	.013	.011
Cl	3	.327	.056	.056
All	220		.035	

No. of molecules = 19;  $r = 0.997$ ;  $m = 0.996$ ;  $b = 0.000$ .

**TABLE XI.**  
**Statistical Results for Magnesium RPS.**

Atom	Number	Avg. abs. charge	Avg. abs. deviation	Avg. signed deviation
H	155	.430	.023	−.008
C	10	.150	.048	−.045
N	13	.974	.063	−.023
O	55	1.002	.042	.011
F	6	.598	.041	−.041
Mg	28	1.435	.133	.072
P	8	.217	.084	−.084
S	7	.313	.062	.031
Cl	9	.221	.062	.040
All	291		.044	

No. of molecules = 28;  $r = 0.996$ ;  $m = 0.987$ ;  $b = 0.000$ .

**TABLE XII.**  
**Statistical Results for Potassium RPS.**

Atom	Number	Avg. abs. charge	Avg. abs. deviation	Avg. signed deviation
H	158	.378	.022	.005
C	5	.439	.142	.121
N	8	1.007	.044	-.028
O	78	.880	.048	-.002
F	1	.570	.035	.035
P	7	.265	.079	-.079
S	3	.467	.034	.034
Cl	2	.331	.050	.050
K	22	.933	.036	.003
All	284		.035	

No. of molecules = 22;  $r = 0.997$ ;  $m = 0.994$ ;  $b = 0.001$ .

hydrogen is the most common atom in both data sets, and is thus weighted more heavily in the error function minimization. In addition, the metal complexes discussed here all have hydrogens on the outside, whereas heavy atoms are buried in the interior. This naturally leads to less well-determined charges for the interior atoms, because the ESP is sampled much more densely around the exterior atoms.<sup>41</sup> Errors for nonhydrogen atoms are uniformly higher than in part I, but this is in part due to the much higher absolute charges found in the metal complexes as opposed to the nonmetal systems dealt with earlier. If fact, if the ratio  $R = (\text{average absolute error})/(\text{average absolute charge})$  is used as a measure of accuracy, the charges for H, O, F, and S are significantly better

determined in the metal complexes than in the molecules in part I, whereas the errors are about the same for N and Cl. Only C, P, and Br show somewhat larger errors in the metal systems. It is gratifying that N and O exhibit reasonable behavior in these metal complexes, because they are by far the most common atoms involved in bonding to metal ions in biological systems. For the metals themselves, the ratio  $R$  (defined earlier) varies from 3.8% (K) to 10.6% (Li) and averages 7.4%.

The statistical results for iodine (Table XV) are similar in all respects to other halogens parameterized earlier.<sup>13</sup> The average absolute error for iodine in the iodine RPS is only  $0.025e^-$ , although the  $R$  ratio is 20%, reflecting the fact that the average iodine charge is very small.

**TABLE XIII.**  
**Statistical Results for Calcium RPS.**

Atom	Number	Avg. abs. charge	Avg. abs. deviation	Avg. signed deviation
H	115	.457	.016	.001
C	6	.366	.079	-.046
N	9	1.051	.044	-.011
O	56	.991	.062	-.016
F	1	.681	.062	-.062
P	2	.543	.029	.013
S	3	.611	.065	.049
Cl	4	.334	.034	.034
Ca	20	1.744	.089	.028
All	216		.039	

No. of molecules = 20;  $r = 0.997$ ;  $m = 0.989$ ;  $b = 0.002$ .

TABLE XIV.  
Statistical Results for Zinc RPS.

Atom	Number	Avg. abs. charge	Avg. abs. deviation	Avg. signed deviation
H	169	.438	.026	-.002
C	10	.426	.113	.041
N	23	1.013	.089	-.077
O	66	.923	.050	.005
F	2	.609	.032	.032
P	3	.283	.112	-.112
S	4	.312	.118	-.065
Cl	5	.386	.154	.141
Zn	32	1.314	.119	.068
Br	2	.273	.170	-.170
All	316		.053	

No. of molecules = 32;  $r = 0.994$ ;  $m = 0.981$ ;  $b = -0.001$ .

The overall statistical results for all 166 molecules in this article are reported in Table XVI. *PESP* achieves an overall absolute average deviation of  $0.042e^-$ , with a correlation coefficient of 0.996. The linear least-squares parameters are  $\mathbf{m} = 0.991$  and  $\mathbf{b} = 0.003$ , demonstrating that scaling is not required to bring *PESP* charges into optimal agreement with the underlying *ab initio* results. The use of a scaling factor is always a disadvantage, because one must assume a universal scaling factor for all molecules, and there is good evidence that such an assumption is unwarranted.<sup>15</sup> Table XVII shows a similar statistical analysis, including

all of the molecules from part I and the current work. For 311 molecules containing 2488 atoms, *PESP* produces an average absolute error of  $0.040e^-$  and a correlation coefficient of 0.995. The range of ESP-derived charges for this data set is  $+2.04$  to  $-1.53e^-$ . A plot of this entire data set is shown in Figure 3.

Detailed timing statistics for several molecules were presented in part I of the series.<sup>13</sup> Here, one typical example is presented. For  $Mg(OH_2)_5(\text{pyridine})^{2+}$  on an HP-735 workstation, *PESP* requires 19.4 seconds of cpu time for the calculation of the wave function and the ESP-derived atomic charges.

TABLE XV.  
Statistical Results for Iodine RPS.

Atom	Number	Avg. abs. charge	Avg. abs. deviation	Avg. signed deviation
H	42	.192	.024	.003
C	39	.374	.054	.017
N	3	.549	.059	-.021
O	7	.378	.035	-.033
F	1	.081	.001	.001
P	1	.096	.076	-.076
S	1	.169	.000	.000
Cl	2	.010	.016	-.013
Br	4	.072	.035	-.002
I	29	.124	.022	-.009
All	117		.034	

No. of molecules = 26;  $r = 0.990$ ;  $m = 1.004$ ;  $b = -0.009$ .

**TABLE XVI.**  
**Statistical Results for All Molecules in Tables I–VII.**

Atom	Number	Avg. abs. charge	Avg. abs. deviation	Avg. signed deviation
H	873	.401	.023	.000
Li	19	.847	.090	–.003
C	89	.318	.065	–.006
N	81	.960	.068	–.035
O	354	.925	.049	.002
F	16	.548	.036	–.014
Na	19	.939	.061	–.001
Mg	28	1.435	.133	.072
P	28	.245	.094	–.091
S	24	.391	.056	.008
Cl	28	.279	.065	.052
K	22	.933	.036	.003
Ca	20	1.744	.089	.028
Zn	32	1.314	.119	.068
Br	6	.139	.078	–.043
I	29	.124	.025	–.009
All	1668		.042	

No. of molecules = 166;  $r = 0.996$ ;  $m = 0.991$ ;  $b = 0.002$ .

**TABLE XVII.**  
**Statistical Results for All Molecules.<sup>a</sup>**

Atom	Number	Avg. abs. charge	Avg. abs. deviation	Avg. signed deviation
H	1172	.351	.022	.000
Li	19	.847	.090	–.003
C	307	.323	.059	–.005
N	143	.822	.060	–.013
O	463	.813	.045	.003
F	51	.274	.030	–.014
Na	19	.939	.061	–.001
Mg	28	1.435	.133	.072
P	49	.321	.083	–.056
S	46	.386	.062	–.001
Cl	61	.233	.052	.028
K	22	.933	.036	.003
Ca	32	1.314	.119	.068
Br	27	.107	.040	–.015
I	29	.124	.022	–.009
All	2488		.040	

No. of molecules = 311;  $r = 0.995$ ;  $m = 0.992$ ;  $b = 0.001$ .

<sup>a</sup> Includes all molecules from part I (see text).

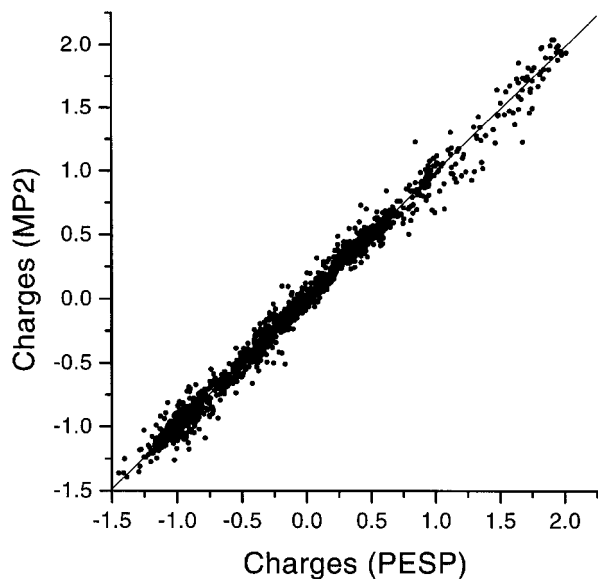


**FIGURE 3.** Plot of *PESP* atomic charges vs. ESP-derived atomic charges from *ab initio* MP2/6-31G\*\* wave functions for all 2488 atoms in the data sets of the present work and part I.<sup>13</sup>

The corresponding times using Gaussian-94 are 203 seconds (HF/STO-3G) and 3924 seconds (HF/6-31G\*). Calculations at the MP2/6-31G\*\* level would, of course, require much more cpu time.

## Conclusions

The *PESP* method has been extended to the metal ions  $\text{Li}^+$ ,  $\text{Na}^+$ ,  $\text{Mg}^{2+}$ ,  $\text{K}^+$ ,  $\text{Ca}^{2+}$ , and  $\text{Zn}^{2+}$ . It represents the first non-*ab initio* approach to be applicable to a wide variety of elements and comparable in accuracy to much more expensive *ab initio* methods.

Extensions of this method are now in progress. In particular, modifications are under development that should result in even more accurate charges, especially for biological systems. This will be accomplished by parameterizing against a new, larger data set with extensive additions of amino acids, sugars, and biologically important anions. In addition, an approach for obtaining ESP-derived charges for whole proteins based on the *PESP* method has now been developed.<sup>42</sup>

## Acknowledgments

The author thanks the Swiss Center for Scientific Computing and Dr. Djordje Maric for a generous grant of cpu time required for the calculation of the *ab initio* ESP-derived charges at the MP2 level.

## References

1. E. Scrocco and J. Tomasi, *Adv. Quantum Chem.*, **11**, 115 (1978).
2. P. Politzer and J. S. Murray, in *Reviews of Computational Chemistry*, Vol. 2, K. B. Lipkowitz and D. B. Boyd, Eds., VCH, New York, ch. 7.
3. P. Politzer and D. G. Truhlar, Eds., *Chemical Applications of Atomic and Molecular Electrostatic Potentials*, Plenum, New York, 1981.
4. G. Náray-Szabó, *Chemical Design Automation News*, **8**, 43 (1993).
5. J. G. Ángyán and G. Náray-Szabó, in *Theoretical Models of Chemical Bonding, Part 4, Theoretical Treatment of Large Molecules and Their Interactions*, Z. B. Maksic, Ed., Springer, Berlin, 1991, p. 1.
6. J. E. Douglas and P. A. Kollman, *J. Am. Chem. Soc.*, **102**, 4295 (1980).
7. G. Pepe, D. Siri, and J.-P. Reboul, *J. Mol. Struct. Theochem*, **14**, 289 (1981).
8. H. Weinstein, R. Osman, and J. P. Green, in *Computer Assisted Drug Design (ACS Symposium Series 112)*, E. C. Olson and R. E. Christoffersen, Eds., American Chemical Society, Washington, DC, 1979.
9. F. A. Momany, *J. Phys. Chem.*, **85**, 592 (1978).
10. S. R. Cox and D. E. Williams, *J. Comput. Chem.*, **2**, 304 (1981).
11. C. M. Breneman and K. B. Wiberg, *J. Comput. Chem.*, **11**, 361 (1990).
12. C. I. Bayly, P. Cieplak, W. D. Cornell, and P. A. Kollman, *J. Phys. Chem.*, **97**, 10269 (1993).
13. D. S. Marynick, *J. Comput. Chem.*, **18**, 955 (1997).
14. B. H. Besler, K. M. Merz Jr., and P. A. Kollman, *J. Comput. Chem.*, **11**, 431 (1990).
15. K. M. Merz Jr., *J. Comput. Chem.*, **13**, 749 (1992).
16. G. P. Ford and B. Wang, *J. Comput. Chem.*, **14**, 1101 (1993).
17. B. Wang and G. P. Ford, *J. Comput. Chem.*, **15**, 200 (1994).
18. B. Beck, T. Clark, and R. C. Glen, *J. Comput. Chem.*, **18**, 744 (1999).
19. J. E. Wampler, *J. Chem. Inf. Comput. Sci.*, **35**, 617 (1995).
20. T. A. Halgren and W. N. Lipscomb, *J. Chem. Phys.*, **58**, 1569 (1973).
21. T. A. Halgren and W. N. Lipscomb, *Proc. Natl. Acad. Sci. USA*, **69**, 652 (1972).
22. D. S. Marynick and W. N. Lipscomb, *Proc. Natl. Acad. Sci. USA*, **79**, 1341 (1982).
23. A. Derecskei-Kovacs and D. S. Marynick, *Int. J. Quantum Chem.*, **58**, 193 (1996).

24. A. Derecskei-Kovacs, D. E. Woon, and D. S. Marynick, *Int. J. Quantum Chem.*, **61**, 67 (1997).
25. A. Derecskei-Kovacs and D. S. Marynick, *Int. J. Quantum Chem.*, **63**, 1081 (1997).
26. D. S. Marynick, *J. Comput. Chem.*, **18**, 1682 (1997).
27. P.-O. Löwdin, *J. Chem. Phys.*, **18**, 365 (1950).
28. See, for instance: F. U. Axe and D. S. Marynick, *Organometallics*, **6**, 572 (1987); F. U. Axe and D. S. Marynick, *J. Am. Chem. Soc.*, **110**, 3728 (1988); L. M. Hansen and D. S. Marynick, *J. Am. Chem. Soc.*, **110**, 2358 (1988); C. A. Jolly and D. S. Marynick, *J. Am. Chem. Soc.*, **111**, 7968 (1989); L. M. Hansen and D. S. Marynick, *Organometallics*, **8**, 2173 (1989); L. M. Hansen and D. S. Marynick, *Inorg. Chem.*, **29**, 2482 (1990); M. Lawless and D. S. Marynick, *Inorg. Chem.*, **30**, 3547 (1991); J. R. Rogers, O. Kwon, and D. S. Marynick, *Organometallics*, **10**, 2817 (1991); M. Lawless and D. S. Marynick, *J. Am. Chem. Soc.*, **113**, 7513 (1991); P. N. V. Pavan Kumar and D. S. Marynick, *Inorg. Chem.*, **32**, 1857 (1993); J. R. Rogers, T. P. S. Wagner, and D. S. Marynick, *Inorg. Chem.*, **33**, 3104 (1994); J. R. Rogers, C. K. Johnson, and D. S. Marynick, *Inorg. Chem.*, **33**, 4566 (1994).
29. Original program: M. Dupuis, D. Spangler, and J. J. Wendoloski, *National Resource for Computations in Chemistry, Software Catalog, Program QG01*, University of California, Berkeley, CA, 1980; This version: M. W. Schmidt, K. K. Baldridge, J. A. Boatz, S. T. Elbert, M. S. Gordon, J. H. Jensen, S. Koseki, N. Matsunaga, K. A. Nguyen, S. J. Su, T. L. Windus, M. Dupuis, and J. A. Montgomery, *J. Comput. Chem.*, **14**, 1347 (1993).
30. R. Ditchfield, W. J. Hehre, and J. A. Pople, *J. Chem. Phys.*, **54**, 724 (1971); W. J. Hehre, R. Ditchfield, and J. A. Pople, *J. Chem. Phys.*, **56**, 2257 (1972); J. D. Dill and J. A. Pople, *J. Chem. Phys.*, **62**, 2921 (1975); M. M. Francl, W. J. Pietro, W. J. Hehre, J. S. Binkley, M. S. Gordon, D. J. DeFrees, and J. A. Pople, *J. Chem. Phys.*, **77**, 3654 (1982).
31. W. J. Stevens, H. Basch, and M. Krauss, *J. Chem. Phys.*, **81**, 6026 (1984).
32. J. S. Binkley, J. A. Pople and W. J. Hehre, *J. Am. Chem. Soc.*, **102**, 939 (1980); M. S. Gordon, J. S. Binkley, J. A. Pople, W. J. Pietro, and W. J. Hehre, *J. Am. Chem. Soc.*, **104**, 2797 (1982).
33. M. J. Frisch, G. W. Trucks, H. B. Schlegel, P. M. W. Gill, B. G. Johnson, M. A. Robb, J. R. Cheeseman, T. Keith, G. A. Petersson, J. A. Montgomery, K. Raghavachari, M. A. Al-Laham, V. G. Zakrzewski, J. V. Ortiz, J. B. Foresman, C. Y. Peng, P. Y. Ayala, W. Chen, M. W. Wong, J. L. Andres, E. S. Replogle, R. Gomperts, R. L. Martin, D. J. Fox, J. S. Binkley, D. J. Defrees, J. Baker, J. P. Stewart, M. Head-Gordon, C. Gonzalez, and J. A. Pople, *Gaussian-94*, Gaussian, Inc., Pittsburgh, PA, 1995.
34. A. Schafer, H. Horn, and R. Alrich, *J. Chem. Phys.*, **97**, 2571 (1992).
35. W. J. Stevens, H. Basch, M. Krauss, and P. Jasien, *Can. J. Chem.*, **70**, 612 (1992).
36. M. L. Connolly, *J. Appl. Cryst.*, **16**, 540 (1983).
37. U. C. Singh and P. A. Kollman, *J. Comput. Chem.*, **5**, 129 (1984).
38. L. M. Chirlian and M. M. Francl, *J. Comput. Chem.*, **8**, 894 (1987).
39. A. J. H. Wachters, *J. Chem. Phys.*, **52**, 1033 (1970).
40. Basis sets were obtained from the Extensible Computational Chemistry Environment Basis Set Database, Version 1.0, as developed and distributed by the Molecular Science Computing Facility, Environmental and Molecular Sciences Laboratory, which is part of the Pacific Northwest Laboratory, P.O. Box 999, Richland, WA 99352, and funded by the U.S. Department of Energy. The Pacific Northwest Laboratory is a multiprogram laboratory operated by Battelle Memorial Institute for the U.S. Department of Energy under contract DE-AC06-76RLO 1830. Contact David Feller, Karen Schuchardt, or Don Jones for further information.
41. M. M. Francl, C. Carey, L. E. Chrilian, and D. M. Gange, *J. Comput. Chem.*, **17**, 367 (1996).
42. J.-H. Wu and D. S. Marynick, manuscript in preparation; "Quantum Mechanical Study of Polarization Effects on Enzyme-Substrate Interactions," J.-H. Wu and D. S. Marynick, abstracts of the 225th meeting of the American Chemical Society, Dallas TX, 1998 (COMP Paper No. 125).